

## Implementation of Nonlinear Cyclic Constitutive Model with Strain Softening in FLAC

L. Xu <sup>1</sup>, F. Cai <sup>2</sup>, G. Chen <sup>3</sup> C. Takahashi <sup>4</sup>

### ABSTRACT

This paper modifies a nonlinear cyclic constitutive model (i.e., UW model) to consider the strain softening of soils under cyclic loading. The modified nonlinear constitutive model (i.e., UW strain-softening model) is then implemented in FLAC. The implementation is verified by comparing the skeleton curve calculated from numerical triaxial compression test with theoretical one and comparing hysteresis loops between considering and not considering the strain softening. The results show that: 1) the soil strength decreases at the time the plastic shear strain starts to accumulate when considering the strain softening; 2) the proposed strain-softening processing technique can ensure the hysteresis loop is connected continuously to subsequent softening skeleton curve. It can be concluded that the modified nonlinear constitutive model can be used to describe the strain softening behaviors of soils subjected to cyclic loading.

### Introduction

The slope damage induced by earthquake can be generally classified as a limited deformation and a catastrophic failure (Wakai et al., 2010). The latter can be more dangerous than the former because the slope may continue to deform after the earthquake until it collapses. There are a number of slopes with catastrophic failure in previous major earthquake, such as Yokawatashi landslide induced by the 2004 Niigata Chuestu earthquake (Onoue et al., 2006) and Tangjiashan landslide induced by the 2008 Wenchuan earthquake (HU et al., 2009).

Numerical modelling provides an effective mean for examining the mechanism of the catastrophic failure. Wakai et al. (2007, 2010) proposed a nonlinear strain-softening cyclic model by modifying a nonlinear cyclic model presented by Wakai and Ugai (2004) (i.e., UW model). The nonlinear strain-softening model was used in slope stability analysis. The strain-softening behavior of soil during cyclic loading can be reasonably well characterized by this model.

In this paper, a strain-softening processing technique is proposed to modify the UW model that has already been implemented in a fully coupled dynamic effective-stress finite element procedure UWLC (Forum 8 Co. Ltd., 2005). Then, the modified model, i.e., the UW strain-softening (UWS) model, is implemented in the finite difference software FLAC 7.0 (Itasca Consulting Group, 2011). Finally, the implementation is verified by comparing the skeleton curve calculated from numerical triaxial compression test with theoretical one and comparing hysteresis loops between considering and not considering the strain softening.

<sup>1</sup>Institute of Geotechnical Engineering, Nanjing Tech University, Nanjing, China, [xulingyu2008@126.com](mailto:xulingyu2008@126.com)

<sup>2</sup>Department of Environmental Engineering Science, Gunma University, Kiryu, Japan, [feicai@gunma-u.ac.jp](mailto:feicai@gunma-u.ac.jp)

<sup>3</sup>Institute of Geotechnical Engineering, Nanjing Tech University, Nanjing, China, [gxc6307@163.com](mailto:gxc6307@163.com)

<sup>4</sup>Pacific Consultants Co. Ltd. Tokyo, Japan, [chiaki.takahashi@tk.pacific.co.jp](mailto:chiaki.takahashi@tk.pacific.co.jp)

## Formulation of the UWS Model

In this section, the formulation of the UW model (Ugai and Wakai, 2004) implemented in UWLC is first explained. Note that there were also some modifications on the UW model in UWLC with respect to the maximum shear stress, loading function, and stress integration method (Forum 8 Co. Ltd., 2005). Then, the proposed strain-softening processing technique is presented.

### *Definition of Skeleton Curve*

The skeleton curve of stress-strain relationship suggested by Hardin and Drnevich (1972) is used in UW model.

$$\tau = \frac{G_0 \gamma}{1 + G_0 \gamma / \tau_f} \quad (1)$$

where  $\tau$  is the shear stress,  $\gamma$  is the shear strain,  $G_0$  is the initial shear modulus,  $\tau_f$  is the shear strength of soil.  $G_0$  is dependent on the confining pressure of soil and is given as follows:

$$G_0 = G_{0,r} P_a \left( \frac{p'}{P_a} \right)^m \quad (2)$$

where  $G_{0,r}$  is the coefficient of shear modulus,  $p'$  is the mean effective stress,  $m$  is a material constant, and  $P_a$  is atmospheric pressure.  $G_0$  at  $p' = p'_0$  was calculated by  $G_0 = \rho v_s^2$ , where  $p'_0$  is the typical mean effective stress of a soil layer,  $\rho$  is the natural density, and  $v_s$  is the shear wave velocity (Xu et al. 2013).

The shear strength  $\tau_f$  is given as :

$$\tau_f = \frac{\sqrt{3}}{2} (c \cos \varphi + p' \sin \varphi) \left( \cos \Theta - \frac{\sin \Theta \sin \varphi}{\sqrt{3}} \right) / R_f \quad (3)$$

where  $c$  is the cohesion of soil,  $\varphi$  is the internal friction of soil,  $\Theta$  is load angle,  $R_f$  is the failure ratio.

The maximum shear stress  $\bar{\tau}$  and strain  $\bar{\gamma}$  in 3D formulation are expressed in terms of tensor invariant.

$$\bar{\tau}(\sigma_{ij}) = \frac{\sqrt{3J_2}}{2} \quad (4a)$$

$$\bar{\gamma}(\varepsilon_{ij}) = \sqrt{3J'_2} \quad (4b)$$

where  $\sigma_{ij}$  and  $\varepsilon_{ij}$  are the current shear stress and strain tensors, respectively,  $J_2$  and  $J'_2$  are the second and third invariants of deviatoric stress, respectively.

According to Eq. (4), the representative shear stress  $\tau$  and strain  $\gamma$ , used in Eq. (1), can be expressed by the following equation.

$$\tau = \bar{\tau}(\sigma_{ij}) \quad (5a)$$

$$\gamma = \bar{\gamma}(\varepsilon_{ij} - \varepsilon_{ij0}) \quad (5b)$$

where  $\varepsilon_{ij0}$  is the initial shear strain.

### ***Definition of Hysteresis Curve***

The hysteresis curve of stress-strain relationship in UW model is expressed by the following equation.

$$\sigma = \frac{a\gamma^n + G_0\gamma}{1 + b\gamma} \quad (6)$$

where the symbols  $\sigma$  and  $\gamma$  are defined as the shear stress and strain on the hysteresis curve, respectively,  $b$  and  $n$  are material contents,  $a$  is dependent on other variables, as seen in Eq. (8). The damping characteristics are represented by the parameters  $b$  and  $n$ , as discussed in Section 3.2.

$\sigma$  and  $\gamma$  are given as follow:

$$\sigma = \bar{\tau}(\sigma_{ij} - \sigma_{ijA}) \quad (7a)$$

$$\gamma = \bar{\gamma}(\varepsilon_{ij} - \varepsilon_{ijA}) \quad (7b)$$

where  $\sigma_{ijA}$  and  $\varepsilon_{ijA}$  are the stress and strain tensors corresponding to the last unloading point (i.e., point A) ( $\gamma_A$ ,  $\sigma_A$ ), as shown in Figure 1. Point A is the reference point and the coordinate of point A agrees with  $(\bar{\gamma}(\varepsilon_{ijA}), \bar{\tau}(\sigma_{ijA}))$ . Referring to Masing rule, the hysteresis curve is connected to the goal point located at the opposite side of the hysteresis curve (i.e., point B). The coordinate of point B ( $\gamma_B$ ,  $\sigma_B$ ) is equal to  $(-\gamma_A, -\sigma_A)$ .

The value of  $a$  in Eq. (6) is calculated based on the assumption that the hysteresis curve passes points A and B.

$$a = \frac{1}{\gamma_A^n} (\sigma_B (1 + b\gamma_B) - G_0\gamma_B) \quad (8)$$

where

$$\sigma_B = |\bar{\tau}_B - \bar{\tau}_A| \quad (9a)$$

$$\gamma_B = |\bar{\gamma}_B - \bar{\gamma}_A| \quad (9b)$$

Note that the subscript  $B$  in Eqs. (8) and (9) represents any point on the hysteresis curve between points  $A$  and  $B$  shown in Figure 1. If the loading direction is reversed before point  $B$ , say, point  $C$  shown in Figure 1, point  $C$  becomes new reference point  $(\gamma_0, \tau_0)$ .

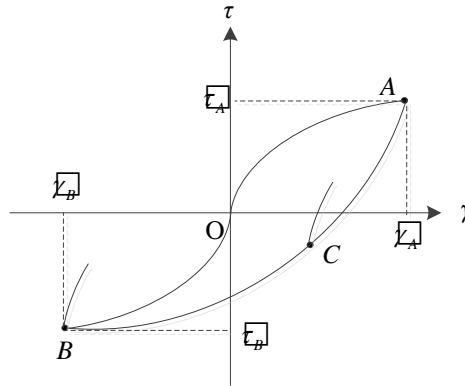


Figure 1 Schematic view of hysteresis loop

### ***The Proposed Strain-Softening Processing Technique***

Figure 2 schematically shows the differences of stress-strain curves between UW model and UWS model. In UW model, the hysteresis curve is connected to the skeleton curve continuously according to Masing rule, as shown by the stress-strain path  $BAC$  in Figure 2. Namely, the hysteresis curve is tangent to the skeleton curve, as shown by tangent point  $A$  in Figure 2. However, in UWS model (Wakai et al., 2007, 2011), the soil strength decreases at the time the plastic shear strain starts to accumulate. Thus, the value of the maximum shear stress at the last unloading point (i.e., point  $A$ ) on the skeleton curve will decrease to that at point  $A'$  shown in Figure 2 when the strain-softening is considered.

To ensure continuous change between hysteresis curve (the stress-strain path  $BA'$  in Figure 2) and subsequent skeleton curve (the stress-strain path  $A'C'$  in Figure 2) in UWS model, the following modifications should be made on the skeleton curve and hysteresis curve.

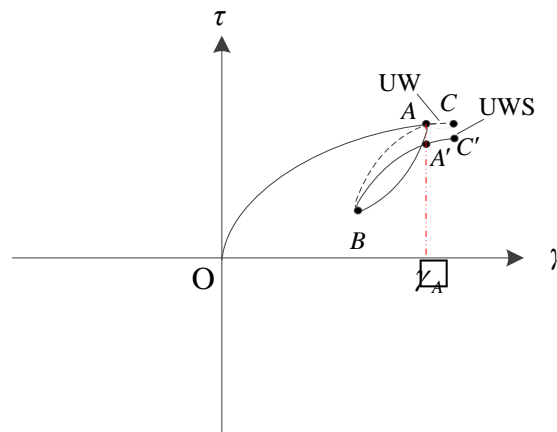


Figure 2 Schematic differences of stress- strain curves between UW and UWS models

### ***Modifications on Skeleton Curve***

The effect of strain-softening of soil on the shear strength  $\tau_f$  is characterized by the following equation suggested by Wakai et al. (2007).

$$\tau_{f,u} = \tau_f + \frac{(R-1)\tau_f}{A + \gamma^p} \gamma^p \quad (10)$$

where  $\tau_{f,u}$  is the updated shear strength,  $R$  is the residual coefficient of shear strength, defined as the residual shear strength  $\tau_{fr}$  divided by the initial shear strength  $\tau_f$ ,  $A$  is a material constant,  $\gamma^p$  is the accumulated plastic shear strain.

The initial shear modulus  $G_0$  is updated based on the updated shear strength  $\tau_{f,u}$ .

$$G_{0,u} = \frac{G_0 \tau_{f,u}}{\tau_f} \quad (11)$$

where  $G_{0,u}$  is the updated shear modulus,  $G_0$  and  $\tau_{f,u}$  are given by Eqs. (2) and (3). Note that  $\tau_{f,u}$  and  $G_{0,u}$  are updated at each time step.

Substituting Eqs. (10) and (11) into Eq. (1) yields the equation

$$\tau = \frac{G_{0,u} \gamma}{1 + G_{0,u} \gamma / \tau_{f,u}} \quad (12)$$

### ***Modifications on Hysteresis Curve***

Substituting Eq. (11) into Eq. (1) yields the equation

$$\mathcal{V}_\sigma = \frac{a \mathcal{V}_\sigma + G_{0,u} \mathcal{V}_\sigma}{1 + b \mathcal{V}_\sigma} \quad (13)$$

Additional modification is necessary for the term  $\mathcal{V}_\sigma$  in Eq. (9a) to consider the effect of strain-softening of soil.

$$\mathcal{V}_{\sigma,u} = \mathcal{V}_\sigma - (\bar{\tau}_A - \bar{\tau}_{A,u}) \quad (14a)$$

where

$$\bar{\tau}_{A,u} = \frac{G_{0,u} \bar{\gamma}_A}{1 + G_{0,u} \bar{\gamma}_A / \tau_{f,u}} \quad (14b)$$

$\mathcal{V}_\sigma$  and  $\bar{\tau}_A$  can be found in Eq. (9a),  $\mathcal{V}_{\sigma,u}$  and  $\bar{\tau}_{A,u}$  are the updated  $\mathcal{V}_\sigma$  and  $\bar{\tau}_A$ , respectively. Eq. (14b) is obtained by substituting  $\bar{\gamma}_A$  into Eq. (10).

## Implementation of UWS Model in FLAC

A mixed discretization technique is used in FLAC. In this technique, each quadrilateral zone (analogous to an element in FEM) is subdivided internally by its diagonals into two overlaid sets of constant-strain triangles. The term “mixed” stems from the fact that different discretizations are used for the isotropic and deviatoric parts of the strain and stress tensor. Isotropic stress and strain components are taken to be constant over the whole quadrilateral element, while the deviatoric components are treated separately for each triangular subzone. Some challenges can be posed to the implementation of highly nonlinear constitutive model by the mixed discretization technique, as reported by Boulanger and Ziotopoulou (2012).

In the present implementation, each subzone has its own memory and develops its own internal variables (e.g., reference stresses and strains, loading direction). This implementation can cause the nonsensical results between the overlapping triangular subzones caused by, as reported Boulanger and Ziotopoulou (2012). However, this implementation is appropriate in this study because only plastic shear strain was considered in UWS model. In contrast, both plastic shear strain and volumetric strain were considered in PM4sand model.

The UWS model is coded in C++ and compiled as a DLL “UWmodel.dll” in Microsoft Visual Studio 2005. The steps required for using a DLL are described in the FLAC manuals. Note that the UW model is automatically triggered by setting the residual strength coefficient  $R = 0$ .

### Verification

To validate the implementation of the UW and UWS models in FLAC program, the simulation of one-zone sample is done by using the unit cell as shown in Figure 3.

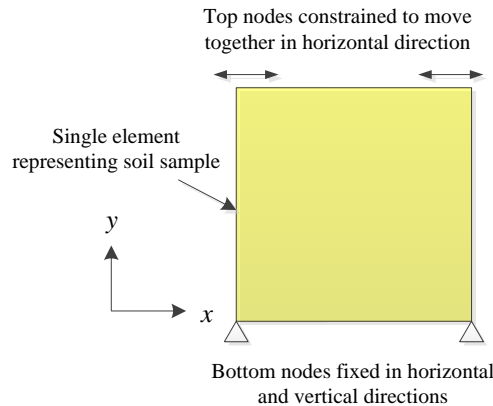


Figure 3 One-zone model in FLAC for simulating monotonic triaxial compression test and cyclic simple shear test (modified after Ebrahimiyan et al. 2013)

Table 1 The parameters of UW or UW strain-softening model

No.	$G_0$ (kPa)	$\nu$ (-)	$c$ (kPa)	$\varphi$ ( $^\circ$ )	$p'$ (kPa)	$b$	$n$	$R_f$	$R$ ( $\tau_{fr}/\tau_f$ )	$A$
1	115385	0.3	24	30.9	60	1316	1.43	0.8	-	-
2	20511	0.49	37	18	67.73	332	2.5	0.8	0.4	2

### Monotonic Triaxial Compression Tests

Monotonic triaxial compression test is modelled using the one-zone model shown in Figure 3. The initial confining pressure is 60 kPa. The UW model was used in the test, of which the input parameters are listed in first line of Table 1. Figure 4 shows the stress-strain relationship calculated from the FLAC program corresponds well with that calculated from theoretical equations as follow.

$$(\sigma_1 - \sigma_3) = \frac{E_0 \varepsilon_1}{1 + E_0 \varepsilon_1 / (\sigma_1 - \sigma_3)_{ult}} \quad (15a)$$

$$E_0 = 2(1 + \nu)G_0 \quad (15b)$$

where  $(\sigma_1 - \sigma_3)$  is maximum principle stress difference,  $\varepsilon_1$  is the axial strain,  $E_0$  is the elastic modulus,  $\nu$  is Poisson ratio, and  $G_0$  is the shear modulus.

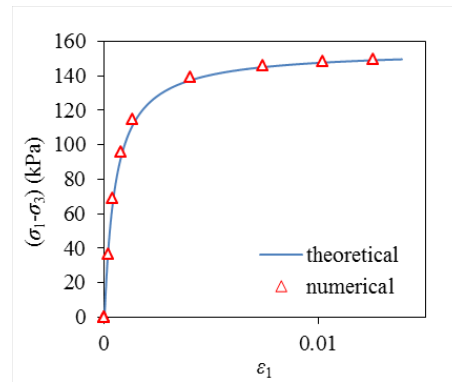
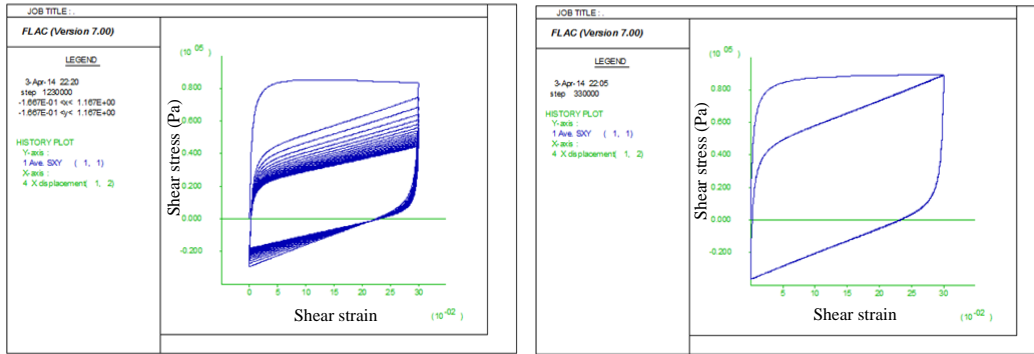


Figure 4 Numerical and theoretical maximum principle stress difference and axial strain relationship

### Cyclic Simple Shear Test

One-zone model shown in Figure 3 is used to simulate cyclic simple shear test to demonstrate the capability of the implemented UWS model. A velocity of  $1e-5$  m/step is applied in the  $x$  axis direction of the top nodes of the one-zone model. The cyclic displacement of the top nodes is controlled in the range of 0 ~ 0.3 m. The shear strain of the unit cell is defined as the cyclic displacement divided by the height of the unit cell, i.e., 1 m. Thus, the cyclic shear strain is in the range of 0 ~ 0.3. The initial confined pressure of the test is 75 kPa. The input parameters for UW and UWS models are listed in the second line of Table 1.

Figs. 5 show the hysteresis loops in a one-zone sample element after about 20 cycles of shaking using UW and UWS models, respectively. The soil strength decreases at the beginning of every hysteresis loop for the UWS model. This is due to the fact that the plastic shear strain accumulates continuously at each time step. In addition, the results using the UWS model show that the shear stress change continuously between different hysteresis loops, as shown in Figure 5(a). As for UW model, all hysteresis loops overlap each other, as shown in Figure 5(b). This indicates that soil strength keeps unchanged during cyclic loading.



(a)

(b)

Figure 5 Hysteresis loop in a one-zone sample element using (a) UWS model and (b) UW model

### Conclusion

In this paper, a strain-softening processing technique is proposed to modify the UW model. Then, the UW strain-softening and UW models are implemented in the finite difference software FLAC 7.0. Finally, the implementation is verified by using one-zone model to simulate the monotonic triaxial compression test and cyclic simple shear test. From the analysis of these two tests, the following conclusion can be obtained:

- (1) The stress-strain relationship calculated from the FLAC program corresponds well with that calculated from theoretical equations.
- (2) The soil strength decreases at the time the plastic shear strain starts to accumulate when considering the strain softening;
- (3) The proposed strain-softening processing technique can ensure the hysteresis loop is connected continuously to subsequent softening skeleton curve.

### Acknowledgments

This research was supported by the National Natural Science Foundation of China (Grant Nos. 51508271, 41172258, 51438004) and the Natural Science Foundation of Jiangsu Province of China (Grant No. SBK2015041778), both of which are gratefully acknowledged.

### References

- Boulangier R W, Ziotopoulou K. *PM4Sand (Version 2): a sand plasticity model for earthquake engineering applications*[J]. Rep. UCD/CGM-12, 2012, 1.
- Ebrahimian B, Mostafavi Moghadam A A, Ghalandarzadeh A. *Numerical Modelling of the Seismic Behaviour of Gravity-Type Quay Walls*[M]. INTECH Open Access Publisher, 2013.
- Forum8 Co. Ltd. *Finite element fully coupled dynamic effective stress analysis program (UWLC)*. Electrical manual, 2005. <http://www.forum8.co.jp/chinese/uc-1/uwlc.htm>?
- Hardin B O, Drnevich V P. Shear modulus and damping in soils. *Journal of the Soil Mechanics and Foundations Division*, 1972, **98**(7): 667-692.



- HU Xiewen, HUANG Runqiu, SHI Yubing et al. Analysis of blocking river mechanism of Tangjiashan landslide and dam-breaking mode. *Chinese Journal of Rock Mechanics and Engineering*, 2009, **28**(1): 181-189 (in Chinese).
- Itasca Consulting Group. *Fast Lagrangian Analysis of Continua*. MN, USA: Itasca Consulting Group, Minneapolis, Minnesota, 2011.
- Onoue A, Wakai A, Ugai K, et al. Slope failures at Yokowatashi and Nagaoka college of technology due to the 2004 Niigata-ken Chuetsu earthquake and their analytical considerations. *Soils and foundations*, 2006, **46**(6): 751-764.
- Pyke R M. Nonlinear soil models for irregular cyclic loadings. *Journal of the Geotechnical Engineering Division*, ASCE, 1979, **105**(GT6):715-726.
- Sloan S W, Booker J R. Removal of singularities in Tresca and Mohr-Coulomb yield functions. *Communications in Applied Numerical Methods*, 1986, **2**(2): 173-179.
- Wakai A, Ugai K, Onoue A, et al. Numerical modeling of an earthquake-induced landslide considering the strain-softening characteristics at the bedding plane. *Soils and foundations*, 2010, **50**(4): 533-545.
- Wakai A, Ugai K. A simple constitutive model for the seismic analysis of slopes and its applications. *Soils and foundations*, 2004, **44**(4): 83-97.
- Wakai A., Ugai K., Onoue A., et al. Finite element simulation for collapse of dip slope during earthquake induced by strain-softening behavior of bedding plane. *Journal of the Japan Landslide Society*, 2007, **44**(3): 145-155(in Japanese).
- Xu L Y, Cai F, Wang G X, et al. Numerical assessment of liquefaction mitigation effects on residential houses: Case histories of the 2007 Niigata Chuetsu-offshore earthquake. *Soil Dynamics and Earthquake Engineering*, 2013, **53**: 196-209.